Conical Spin-Spiral State in an Ultrathin Film Driven by Higher-Order Spin Interactions

Y. Yoshida,[1] S. Schröder,[2,*] P. Ferriani,[2] D. Serrate,[1] A. Kubetzka,[1] K. von Bergmann,[1] S. Heinze,[2] and R. Wiesendanger[1]

[1]*Institute of Applied Physics, University of Hamburg, Jungiusstrasse 11, D-20355 Hamburg, Germany*

[2]*Institute for Theoretical Physics and Astrophysics, Christian-Albrechts-Universität zu Kiel, D-24098 Kiel, Germany*

(Received 14 October 2011; published 22 February 2012)

We report a transverse conical spin spiral as the magnetic ground state of a double-layer Mn on a W(110) surface. Using spin-polarized scanning tunneling microscopy, we find a long-range modulation along the [001] direction with a periodicity of 2.4 nm coexisting with a local row-wise antiferromagnetic contrast. First-principles calculations reveal a transverse conical spin-spiral ground state of this system which explains the observed magnetic contrast. The canting of the spins is induced by higher-order exchange interactions, while the spiraling along the [001] direction is due to frustrated Heisenberg exchange and Dzyaloshinskii-Moriya interaction.

DOI: 10.1103/PhysRevLett.108.087205 PACS numbers: 75.70.Ak, 68.37.Ef, 71.15.Mb, 75.25.−j

Magnetic materials are commonly described based on the Heisenberg model $H = -\sum_{ij} J_{ij} \mathbf{S}_i \cdot \mathbf{S}_j$ with pairwise exchange interaction of strength J_{ij} among spins $\mathbf{S}_i$ and $\mathbf{S}_j$ located on lattice sites i and j, respectively. The Heisenberg model can be obtained as a perturbative expansion of the Hubbard model up to second order in t/U, where t is the hopping matrix element of electrons on the lattice and U is the on-site Coulomb repulsion among electrons. Higher-order terms such as the biquadratic and the four-spin exchange interaction which appear in fourth order [1] are typically neglected in transition metal magnets. In contrast, the significant contribution of the four-spin interaction in nuclear magnetism of solid ^{3}He is well known. Because of the hard core of the interatomic potential in solid ^{3}He, three-body or four-body cyclic exchange is more favorable than direct two-body exchange leading to an exotic antiferromagnetic up-up-down-down ground state [2,3]. Spin interactions beyond the Heisenberg model play an important role also in high-T_C superconductors [4] and spin-liquid states [5], while experimental evidence for its relevance in transition metals is rare, although its importance was theoretically predicted for bulk systems [6,7] as well as ultrathin films [8–10]. Recently, the first film system was reported in which such terms play a role in the formation of a two-dimensionally modulated spin structure at a surface [11].

Here, we report a transverse conical spin-spiral state in an ultrathin film composed of two atomic layers of Mn on W(110). This spin structure is characterized by magnetic moments rotating on a cone that is perpendicular to the [001] propagation direction of the spin spiral with a periodicity of 2.4 nm. The cones of nearest-neighbor Mn atoms point into opposite directions which results in nearly antiferromagnetic alignment. Conical spiral magnetic order, which is known in bulk rare-earth metals and Mn compounds [12], is observed here at the surface for the first time. This intriguing spin structure has been resolved on the atomic scale by using spin-polarized scanning tunneling microscopy (SP STM) and confirmed to be the ground state based on density-functional theory. From our calculations, we conclude that the canting of the spins is driven by higher-order spin interactions, while the Dzyaloshinskii-Moriya and the Heisenberg exchange interaction stabilize the spiraling along the [001] direction.

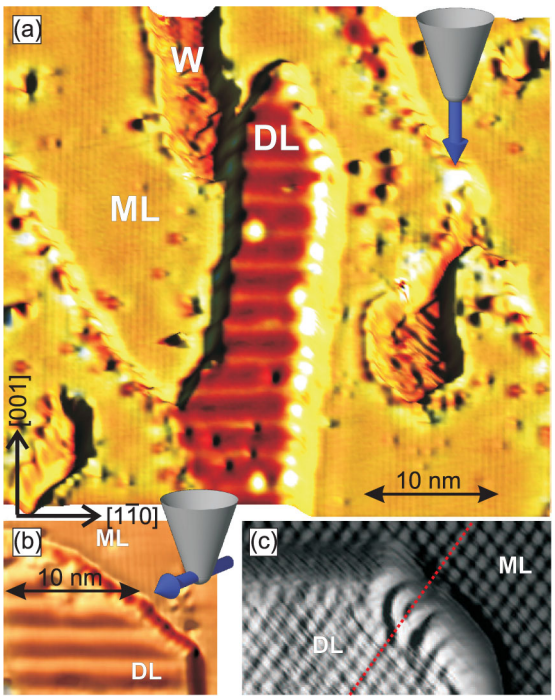

FIG. 1 (color online). Constant-current images of the Mn ML and DL on W(110) colorized with a simultaneously acquired differential conductance signal measured at 9 K with an Fe-coated W tip sensitive to the (a) out-of-plane and (b) in-plane sample magnetization component ($I = 2$ nA, $U = +60$ mV, $B = +2$ T and $U = +10$ mV, $B = 0$ T, respectively). (c) Atomically resolved topography ($I = 2$ nA, $U = -40$ mV, and $B = -2.5$ T). The red line shows the correspondence of atomic positions in the ML and those in the DL, demonstrating pseudomorphic growth.

Figure 1(a) shows a typical SP STM measurement of a sample of 1.15 atomic layers Mn on W(110) obtained with a tip sensitive to the out-of-plane magnetization component (see Supplemental Material [13] for experimental details). The monolayer (ML) areas show the well-known periodic appearance of fine lines along [001] originating from the spin-spiral ground state with an angle of approximately 173° between adjacent atomic rows [14]. The elongated double-layer (DL) island in the center of the image shows pronounced stripes along the $[1\bar{1}0]$ direction with a periodicity of about 2.4 nm. An atomically resolved image of the ML and DL [Fig. 1(c)] shows the pseudomorphic growth of both layers which excludes a structural origin for the stripes on the DL. Instead, we interpret the darker and brighter regions to have magnetization components parallel and antiparallel to the tip magnetization, i.e., pointing up and down with respect to the surface. The measurement shown in Fig. 1(b) with a tip magnetized in the surface plane reveals the same periodic stripes on the DL as obtained with an out-of-plane magnetized tip [Fig. 1(a)]. From these observations alone, we would conclude that the magnetic state of the DL is a spin spiral with magnetic moments rotating in a plane perpendicular to the surface with an angle of ~24° between adjacent atomic rows, similar to the state found for Mn/W(001) [15].

However, a closer look at the Mn DL using a spin-polarized tip with a different in-plane magnetization direction reveals a more complicated scenario. Figure 2(a) displays a constant-current image of the Mn ML (top) and the Mn DL (bottom) connecting at a buried W step edge. As expected, the DL shows the characteristic stripes (horizontal), but with this spin-polarized tip both the ML and the DL exhibit the fine lines indicative of local antiferromagnetic order. Still there is a qualitative difference between the fine lines: While they vanish periodically on the ML due to their origin in the spin spiral, they are strictly periodic on the DL with twice the atomic lattice periodicity.

Based on these additional measurements, we suggest a truly three-dimensional spin state which can be viewed as a superposition of a cycloidal spin spiral along [001] and a $c(2 \times 2)$ antiferromagnetic state with moments aligned along $[1\bar{1}0]$. A sketch of such a state is shown in Fig. 2(b) and can be characterized as a conical spin spiral. Figure 2(c) shows simulations of SP STM images based on the independent orbital approximation [16] for the tip magnetization $\mathbf{m}_T$ along the three principal axes as sketched. The simulated images for a tip with a magnetization perpendicular to the surface or along [001] display the long-range modulation (horizontal stripes) that we also

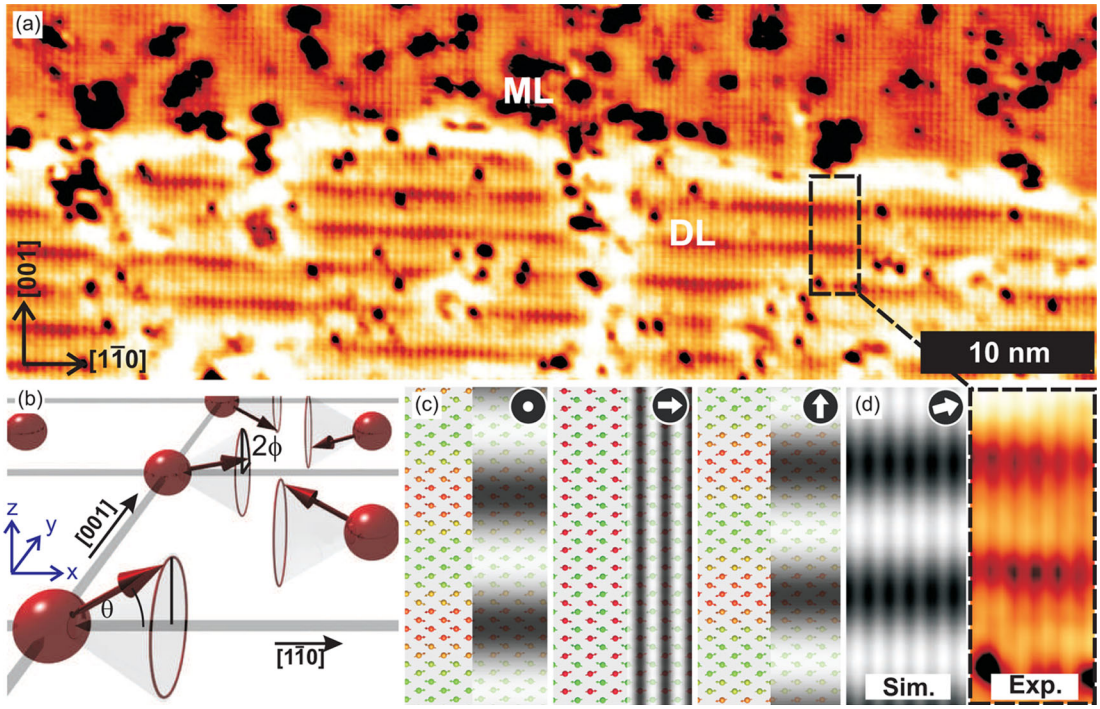

FIG. 2 (color online). (a) Constant-current image of the ML and DL Mn/W(110) with a tip sensitive to the in-plane magnetization component of the sample with a buried W step edge (bright horizontal stripe) ($I = 2$ nA, $U = -10$ mV, $B = 0$ T, and $T = 8$ K). (b) Sketch of a conical spin spiral for the DL Mn/W(110) (only the magnetic moments of the topmost layer are displayed). (c) Simulated SP STM images for different tip magnetization directions superimposed on a ball model of the conical spin structure of (b) for $\theta = 30°$ and $\phi = \phi_{exp} = 24°$. The color scale ranging from red to green indicates the projection of the Mn moments onto the tip magnetization direction (indicated by the white thick arrow). (d) Simulation with an in-plane tip magnetization enclosing an angle of 20° from the $[1\bar{1}0]$ direction and magnified view of the area surrounded by the black broken line in (a).

observed in the measurements shown in Fig. 1. A tip with $\mathbf{m}_T$ along $[1\bar{1}0]$, on the other hand, results in the fine stripe pattern (vertical) observed in Fig. 2. In an experiment without a magnetic field, $\mathbf{m}_T$ will most probably not be aligned perfectly along any of the principal in-plane axes. As shown in Fig. 2(d), a canted tip magnetization leads to a superposition of the long-range modulation and the fine stripe structure that is in excellent agreement with the experiment shown in Fig. 2(a). These simulations demonstrate that the proposed conical spin-spiral state can explain the measurements.

In order to investigate whether this state is the magnetic ground state of the Mn DL on W(110) and to elucidate its microscopic origin we have performed density-functional theory calculations applying the full-potential linearized augmented plane wave method as implemented in the FLEUR code [13,17]. First we focus on the four collinear magnetic configurations sketched in Fig. 3(a): ferromagnetic (FM), layered antiferromagnetic (LAFM), and two row-wise antiferromagnetic structures (RW AFM I and II). In the RW AFM states, a checkerboard antiferromagnetic arrangement of the moments is considered in each Mn layer which can result in either parallel or antiparallel alignment of the moments in each atomic row along the [001] direction. From the total energy differences [see Fig. 3(a)], we can determine the exchange constants up to the third neighbor, namely, the interlayer nearest neighbor $J_1 = -20.6$ meV, the intralayer nearest neighbor $J_2 = -6.9$ meV, and the interlayer next-nearest neighbor $J_3 = -5.2$ meV. These values reveal a strong tendency towards local antiferromagnetic order, consistent with finding the RW AFM II to be the energetically most favorable collinear state. Upon inclusion of spin-orbit coupling, we found the easy magnetization axis in the RW AFM II state to be along the $[1\bar{1}0]$ direction with energy differences of 1.8 and 0.5 meV for a magnetization along [110] and [001], respectively.

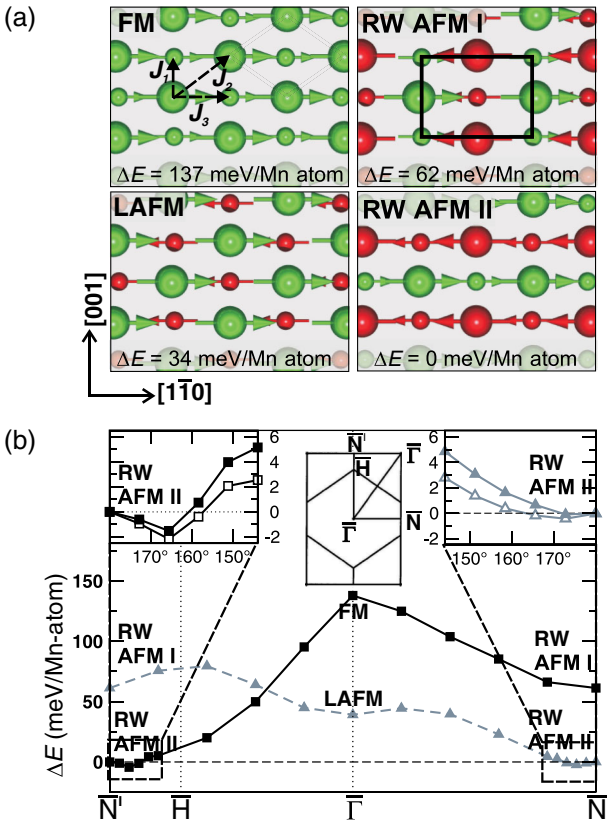

FIG. 3 (color online). (a) Collinear magnetic configurations for the Mn DL on W(110) (top view). Large (small) spheres represent Mn atoms in the surface (subsurface) layer. The position of first, second, and third neighbors is indicated. The employed magnetic unit cell is sketched by a rectangle. (b) Calculated energy dispersion of spin spirals along the $\bar{N}'$-$\bar{H}$-$\bar{\Gamma}$-$\bar{N}$ direction of the two-dimensional Brillouin zone (see the middle inset) starting from the FM (filled squares) and LAFM configuration (filled triangles). The insets show the dispersion curves close to the $\bar{N}'$ and $\bar{N}$ points for a larger k-point cutoff (see [13]), including the Dzyaloshinskii-Moriya interaction (open symbols).

To check for instabilities against noncollinear magnetic order, we have studied the energy dispersion $E(\mathbf{q})$ of flat spin spirals, i.e., states in which the magnetization at atom site $\mathbf{R}_i$ is given by $\mathbf{M}_i = M(0, \cos(\mathbf{q}\cdot\mathbf{R}_i), \sin(\mathbf{q}\cdot\mathbf{R}_i))$, where $\mathbf{q}$ is the vector along which the spin spiral propagates [18]. Starting from the FM and LAFM configurations, we calculated $E(\mathbf{q})$ for $\mathbf{q}$ along the high symmetry lines of the two-dimensional Brillouin zone [Fig. 3(b)]. At the high symmetry points $\bar{N}$ and $\bar{N}'$, we obtain the RW AFM I and RW AFM II state. For spin spirals close to RW AFM II [see the insets in Fig. 3(b)], we found an energy minimum of -1.5 meV/Mn atom corresponding to a spin-spiral state with a rotation angle of 166° between magnetic moments of adjacent atoms along the [001] direction. This is not in accordance with the experimental results, but the observed instability shows a tendency towards noncollinearity due to frustrated exchange interactions [15]. The Dzyaloshinskii-Moriya interaction (DMI) modifies the energetics only slightly as seen in the insets and does not change the physical picture.

Finally, we consider the conical spin spiral suggested by the experiment [cf. Fig. 2(b)]. As it is the superposition of a spin spiral and an antiferromagnetic configuration, such a state has to be calculated by including two Mn atoms per layer in the unit cell as shown in Fig. 4. As a first step, we consider only a canting of the spins by an angle θ starting from the RW AFM II state. The magnetic moments in the two Mn layers can be canted in the same or in the opposite direction which leads to configuration I or II, respectively, as shown in Figs. 4(a) and 4(b). Upon canting the moments [Fig. 4(c)], we obtain an energy minimum at $\theta = 30°$ for configuration I, which is by 10.0 meV/Mn atom lower than the RW AFM II state, whereas configuration II gains only about 5.1 meV/Mn atom.

Analyzing the energy contribution from the Heisenberg exchange for all neighbors upon canting of the magnetic moments, we find that $E_{\text{exch}}(\theta) \propto \cos 2\theta$; i.e., it is minimized for collinear magnetic configurations. Therefore, the

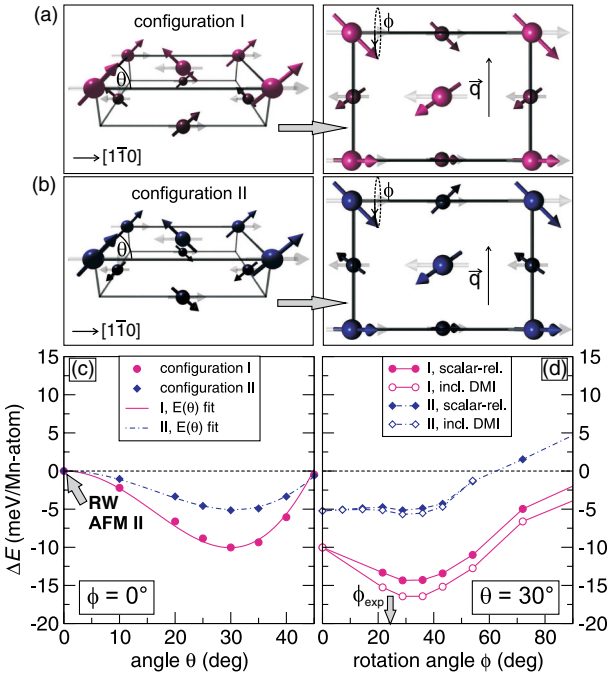

FIG. 4 (color online). (a),(b) Configurations I and II are obtained from the RW AFM II state [see Fig. 3(a)] by canting the magnetic moments by an angle θ. Adding a rotation angle ϕ along [001] gives a conical spin spiral. (c) Total energy of configurations I and II with respect to the RW AFM II state as a function of θ. Symbols (lines) denote results of (fits to) the calculations. (d) Total energy with respect to the RW AFM II state as a function of ϕ for $\theta = 30°$. Open circles denote calculations including the DMI.

pairwise Heisenberg exchange cannot explain the energy minima observed in our first-principles calculations, which implicitly contain all magnetic interactions within the exchange-correlation potential. Since the magnetic moments of the Mn atoms are nearly constant upon canting and since the spin-orbit coupling has been neglected, we attribute the energy gain for noncollinear configurations to higher-order spin interactions. The energy contribution due to nearest-neighbor biquadratic and four-spin interaction scales with $E_{\mathrm{higher}}(\theta) \propto \cos 4\theta$, which can favor noncollinear magnetic states and can explain the energy decrease due to canting of the magnetic moments. The fit of the calculated energies with the $\cos 2\theta$ term due to Heisenberg exchange and the $\cos 4\theta$ term due to higher-order interactions is excellent, as shown in Fig. 4(c). The larger energy gain for this noncollinear structure as compared to the case of flat spin-spirals [cf. the inset in Fig. 3(b)] is a signature of the importance of the higher-order terms for this system.

Based on the optimum canting angle $\theta = 30°$, we considered a homogeneous rotation of the component of the magnetic moments on a cone as sketched in Fig. 2(b) by an angle ϕ from one atom to the next along the [001] direction. In the case of configuration I, we observe an additional energy gain of about 4.6 meV/Mn atom for $\phi = 32°$ corresponding to a period length of $\lambda = 1.8$ nm in reasonable agreement with the measurements, whereas configuration II loses energy upon increasing ϕ. Including the DMI again lowers the energy of the minimum of configuration I by 2.1 meV/Mn atom. This shows that the Mn DL on W(110) exhibits a conical spin spiral along [001] with unique rotational sense and antiparallel [1$\bar{1}$0] magnetization components of nearest neighbors.

It is our pleasure to thank Gustav Bihlmayer for many insightful discussions, Matthias Menzel for technical assistance, HLRN for providing computational time, and the SFB668, the ERC Advanced Grant FURORE, and the Landesexzellenzcluster NANOSPINTRONICS for financial support.

*Corresponding author.
schroeder@theo-physik.uni-kiel.de

[1] A. H. MacDonald, S. M. Girvin, and D. Yoshioka, Phys. Rev. B **37**, 9753 (1988).
[2] D. D. Osheroff, M. C. Cross, and D. S. Fisher, Phys. Rev. Lett. **44**, 792 (1980).
[3] M. Roger, J. H. Hetherington, and J. M. Delrieu, Rev. Mod. Phys. **55**, 1 (1983).
[4] R. Coldea, S. M. Hayden, G. Aeppli, T. G. Perring, C. D. Frost, T. E. Mason, S.-W. Cheong, and Z. Fisk, Phys. Rev. Lett. **86**, 5377 (2001).
[5] F. L. Pratt, P. J. Baker, S. J. Blundell, T. Lancaster, S. Ohira-Kawamura, Y. Baines, C. Shimizu, K. Kanoda, I. Watanabe, and G. Saito, Nature (London) **471**, 612 (2011).
[6] S. Lounis and P. H. Dederichs, Phys. Rev. B **82**, 180404 (2010).
[7] R. Singer, F. Dietermann, and M. Fähnle, Phys. Rev. Lett. **107**, 017204 (2011).
[8] P. Kurz, G. Bihlmayer, K. Hirai, and S. Blügel, Phys. Rev. Lett. **86**, 1106 (2001).
[9] P. Ferriani, I. Turek, S. Heinze, G. Bihlmayer, and S. Blügel, Phys. Rev. Lett. **99**, 187203 (2007).
[10] B. Hardrat, A. Al-Zubi, P. Ferriani, S. Blügel, G. Bihlmayer, and S. Heinze, Phys. Rev. B **79**, 094411 (2009).
[11] S. Heinze, K. von Bergmann, M. Menzel, J. Brede, A. Kubetzka, R. Wiesendanger, G. Bihlmayer, and S. Blügel, Nature Phys. **7**, 713 (2011).
[12] S. DiNapoli, A. M. Llois, G. Bihlmayer, S. Blügel, M. Alouani, and H. Dreyssé, Phys. Rev. B **70**, 174418 (2004).
[13] See Supplemental Material at http://link.aps.org/supplemental/10.1103/PhysRevLett.108.087205 for details of the calculation.
[14] M. Bode, M. Heide, K. von Bergmann, P. Ferriani, S. Heinze, G. Bihlmayer, A. Kubetzka, O. Pietzsch, S. Blügel, and R. Wiesendanger, Nature (London) **447**, 190 (2007).
[15] P. Ferriani, K. von Bergmann, E. Y. Vedmedenko, S. Heinze, M. Bode, M. Heide, G. Bihlmayer, S. Blügel, and R. Wiesendanger, Phys. Rev. Lett. **101**, 027201 (2008).
[16] S. Heinze, Appl. Phys. A **85**, 407 (2006).
[17] http://www.flapw.de.
[18] P. Kurz, F. Förster, L. Nordström, G. Bihlmayer, and S. Blügel, Phys. Rev. B **69**, 024415 (2004).